Electronic Supplementary Material (ESI) for Journal of Materials Chemistry A.

Supporting Information

Zeolite Y Microspheres with Perpendicular Mesochannels and Metal@Y Heterostructures for Catalytic and SERS Applications

Zhuwen Chen,[‡] Chao Chen,[‡] Jian Zhang, Guangchao Zheng, Yanding Wang, Lei Dong, Wei Qian, Shan Bai, Mei Hong[*]

Guangdong Provincial Key Laboratory of Nano-Micro Materials Research, School of Chemical Biology & Biotechnology, Peking University Shenzhen Graduate School, Shenzhen 518055, China.

* E-mail: hongmei@pkusz.edu.cn

[‡] These authors contributed equally.

Table S1. Particle characteristics of NaY microsphere samples synthesized with various additives.

Entry Number	Additive[a]	Chemical Structure	pKa（25 °C）	Boiling Point (°C)	NaY Particle Size (μm)	NaY Yield (g)
1	H_2O		15.7	100	0.680±0.086	3.70
2	Methanol		15.2	65.4	1.554±0.153	3.71
3	Methanol[b]		15.2	65.4	1.730±0.169	3.69
4	Ethanol		16	78	1.471±0.140	3.53
5	n-propanol	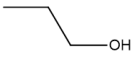	pH=7	97	1.275±0.165	3.54
6	Isopropanol	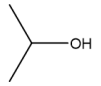	17.1	82	1.194±0.150	3.63
7	n-butanol	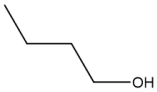	pH=7	117.6	0.975±0.090	3.67
8	tert-butanol		19	83	0.960±0.109	3.71
9	Ethylene glycol	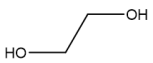	14.22	196-198	1.281±0.220	3.54
10	Glycerol	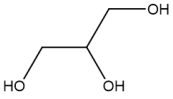	14.15	290	1.236±0.181	2.72
11	tert-butanol[c]		19	83	1.144±0.108	3.62
12	tert-butanol[d]		19	83	1.477±0.137	3.75

[a]alcohol/silica molar ratio =1, [b]methanol amount doubled to methanol/silica molar ratio of 2, [c]*tert*-butanol amount doubled to *tert*-butanol/silica molar ratio of 2, [d]in the co-presence of L-carnitine with LC/silica ratio of 0.2.

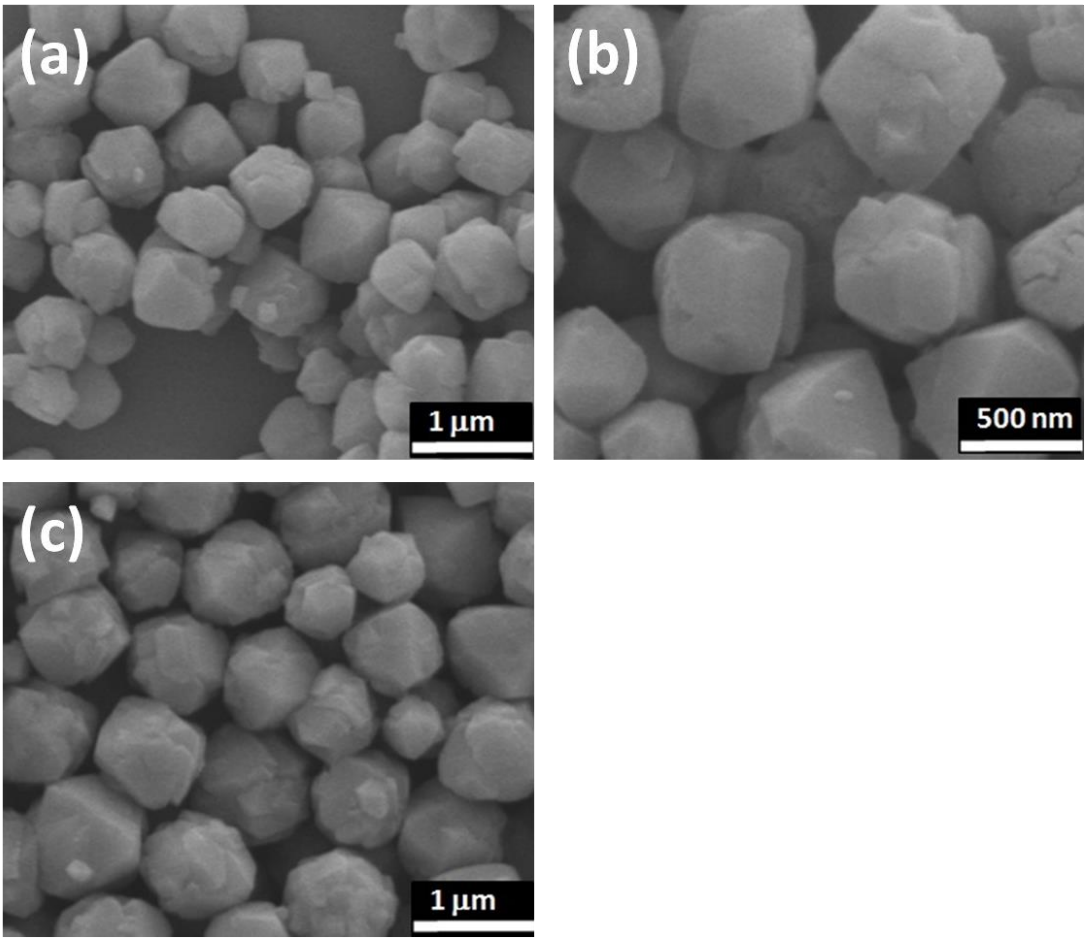

Figure S1. SEM images of samples (a) CFAU, (b) CFAU-LT, (c) CFAU-LT-Pd^{2+}.

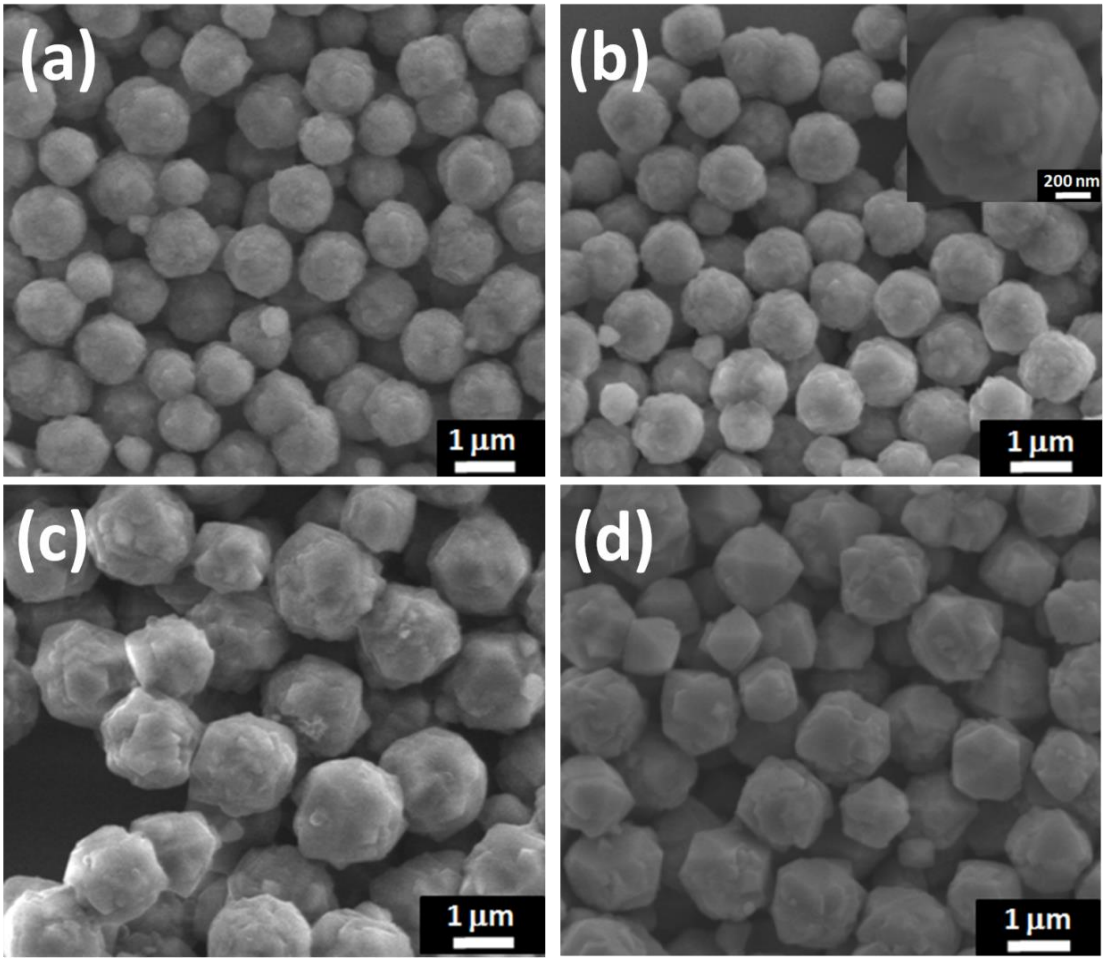

Figure S2. SEM images of FAU samples synthesized in the presence of (a) *tert*-butanol with alcohol/silica ratio of 1, (b) *tert*-butanol with alcohol/silica ratio of 2, (c) methanol with alcohol/silica ratio of 2, (d) *tert*-butanol with synthesis temperature of 100 °C.

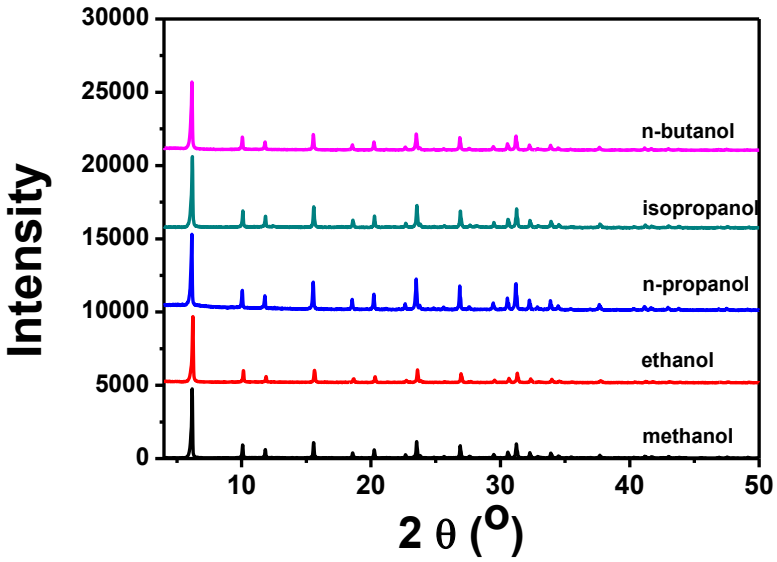

Figure S3. XRD patterns of MFAU crystals synthesized in the presence of various mono-alcohol modifers.

Table S2. Textural properties of as-made samples.

Sample	Surface Area (m^2/ g)			Pore Volume (cm^3/ g)		
	S_{total}[a]	S_{micro}[b]	S_{ext}[c]	V_{total}[d]	V_{micro}[e]	V_{meso}[f]
CFAU	608	565	43	0.34	0.31	0.03
CFAU-Pd^{2+}	588	529	59	0.34	0.29	0.05
CFAU-LT	598	494	104	0.33	0.26	0.07
CFAU-LT-Pd^{2+}	559	448	111	0.34	0.24	0.10
MFAU-TB	658	614	44	0.36	0.33	0.03
MFAU-TB-LT	607	494	113	0.36	0.26	0.10
MFAU-TB-LT-Pd^{2+}	553	433	120	0.35	0.23	0.12
CFAU-LC	658	617	41	0.34	0.32	0.02
CFAU-LC-LT	693	601	92	0.37	0.32	0.05
MFAU-TBLC	650	609	41	0.34	0.32	0.02
MFAU-TBLC-LT	602	461	141	0.37	0.24	0.13
MFAU-TBLC-LT-Pd^{2+}	555	409	146	0.37	0.23	0.14
Ag@MFAU	592	454	138	0.36	0.24	0.12

[a]BET surface area.

[b]*t*-Plot micropore surface area.

[c]*t*-Plot external surface area.

[d]Total pore volume of pores calculated at P/P_o = 0.98

[e]*t*-Plot micropore volume.

[f]$V_{meso} = V_{total}-V_{micro}$

Table S3. SiO_2/Al_2O_3 ratio and metal content in as-made samples.

Sample	SiO_2/Al_2O_3[a]	Metal (%)[b]
CFAU	3.41	-
CFAU-Pd^{2+}	3.45	2.02
CFAU-LT	3.84	-
CFAU-LT-Pd^{2+}	3.94	1.89
CFAU-LC	3.55	-
CFAU-LC-LT	4.28	-
MFAU-TB	3.50	-
MFAU-TB-LT	4.02	-
MFAU-TB-LT-Pd^{2+}	4.04	2.10
MFAU-TBLC	3.46	-
MFAU-TBLC-LT	4.20	-
MFAU-TBLC-LT-Pd^{2+}	4.20	2.20
Ag@MFAU	4.28	5.36
Ag@CFAU	3.91	5.28

[a]SiO_2/Al_2O_3 ratio determined by EDX.
[b]Metal content measured by ICP.

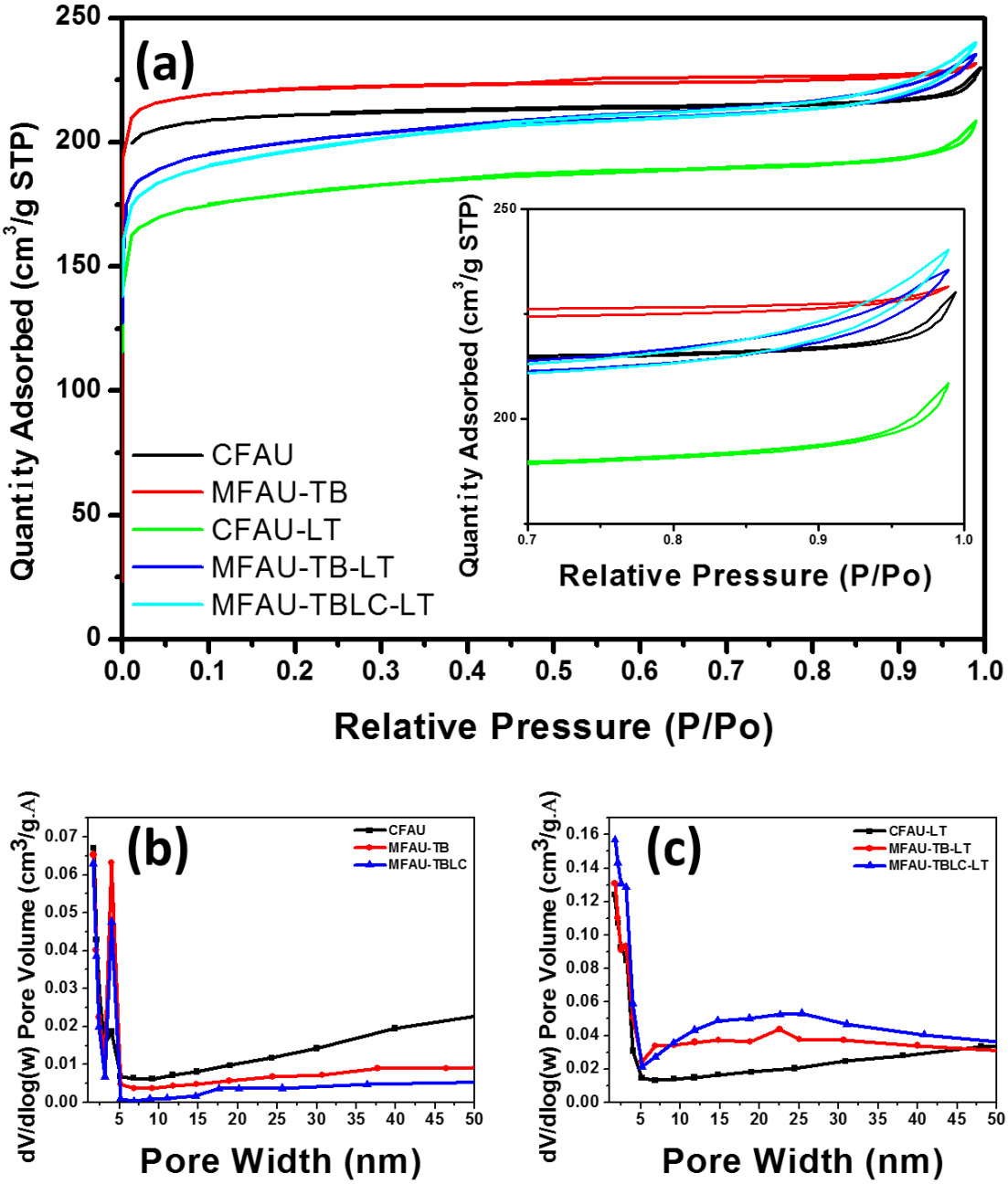

Figure S4. (a) N_2 adsorption-desorption isotherms of as-made samples. Inset is the zoomed-in isotherms at P/P_0 between 0.7-1.0 showing obvious *H3* hysteresis loops especially for MFAU-TBLC-LT. (b-c) BJH mesopore size distribution corresponding to the desorption branch.

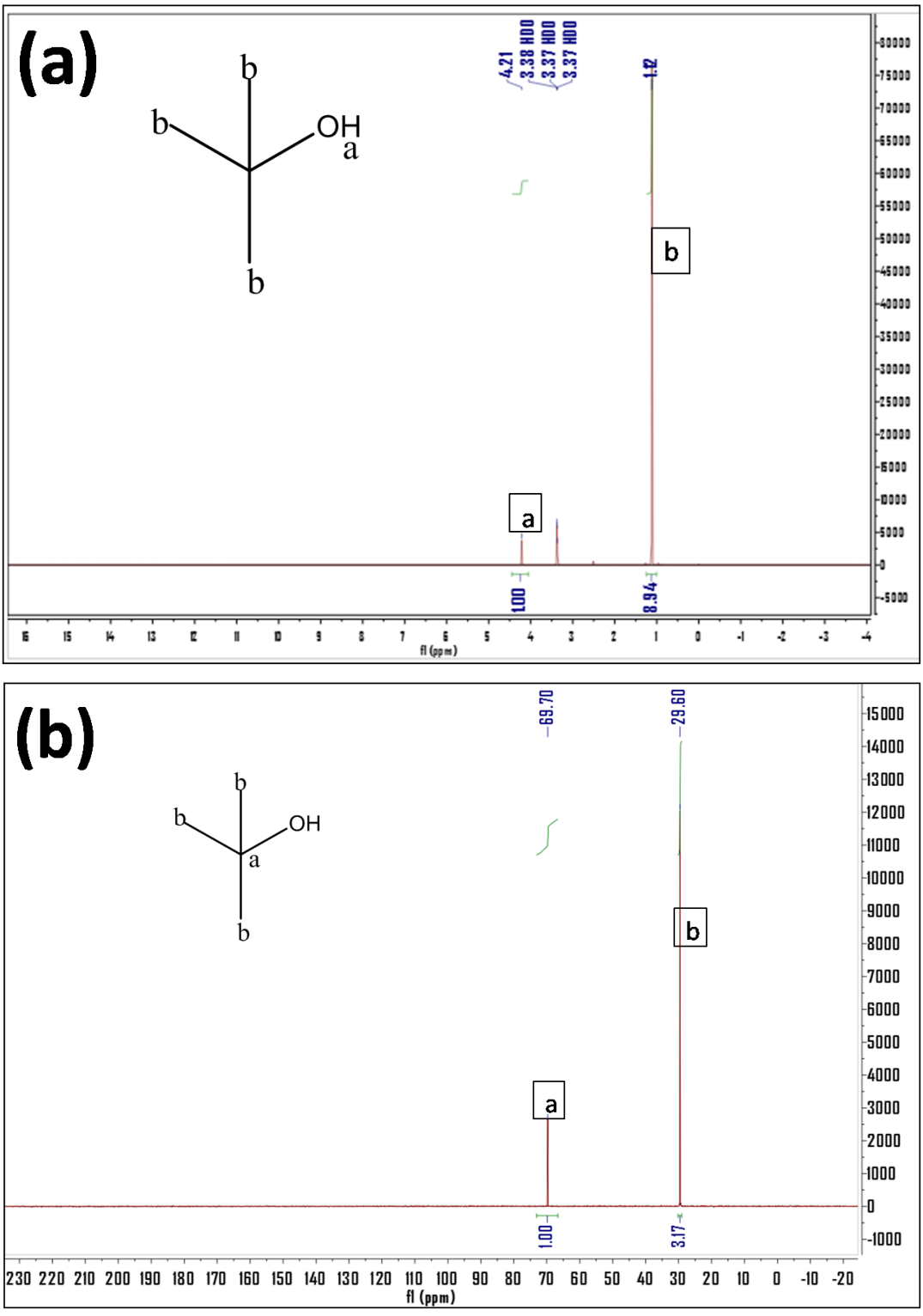

Figure S5. (a) ^{1}H-NMR and (b) ^{13}C-NMR of recovered tert-butanol after the zeolite microsphere synthesis process. Samples were dissolved in deuterated DMSO for ^{1}H-NMR measurement, and in deuterated H_2O for ^{13}C-NMR measurement.

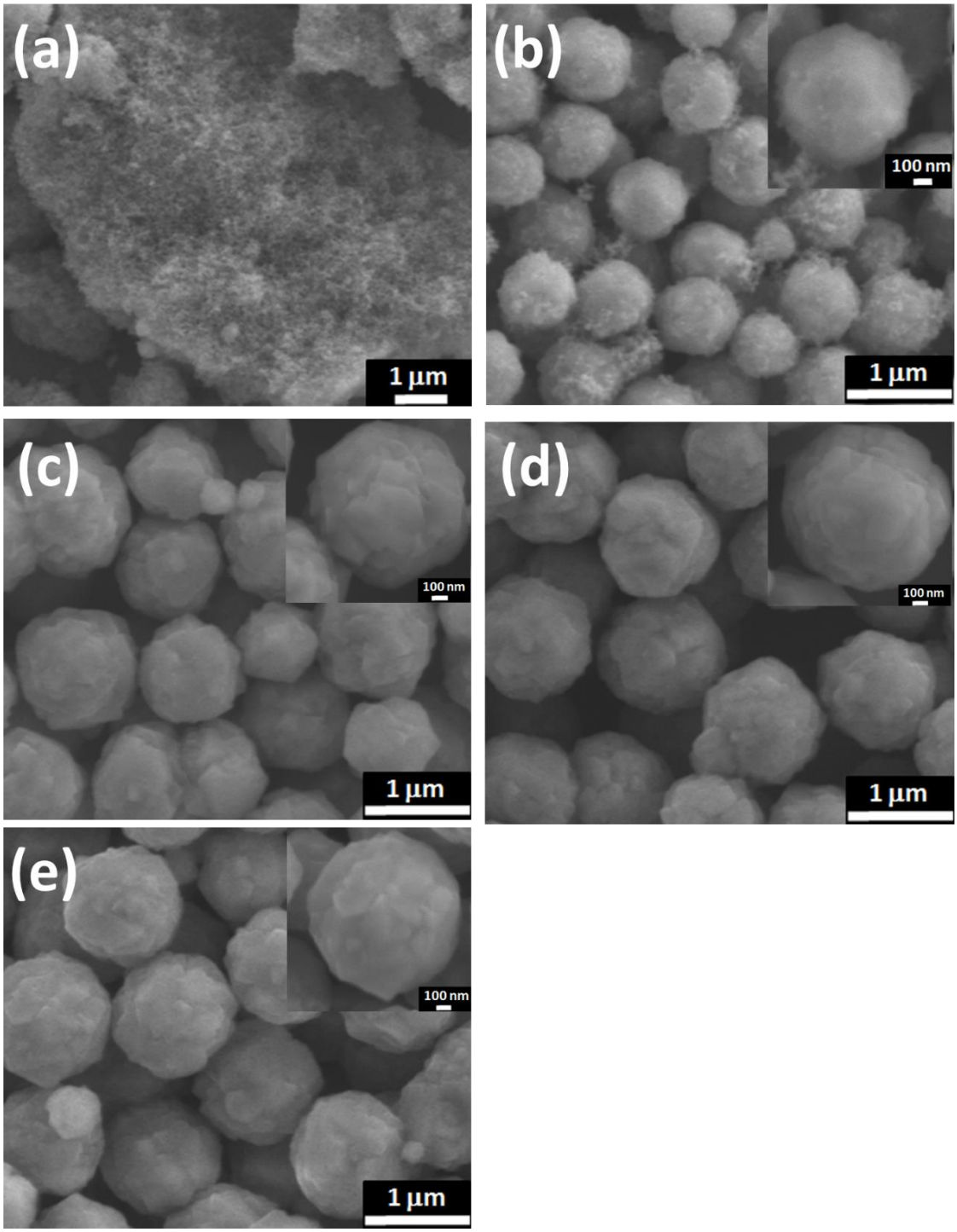

Figure S6. SEM images of MFAU-TB samples at different synthesis stage of (a) 12 h, (b) 24 h, (c) 36 h, (d) 44 h, (e) 48 h. The inset images at higher magnification show surface features of samples.

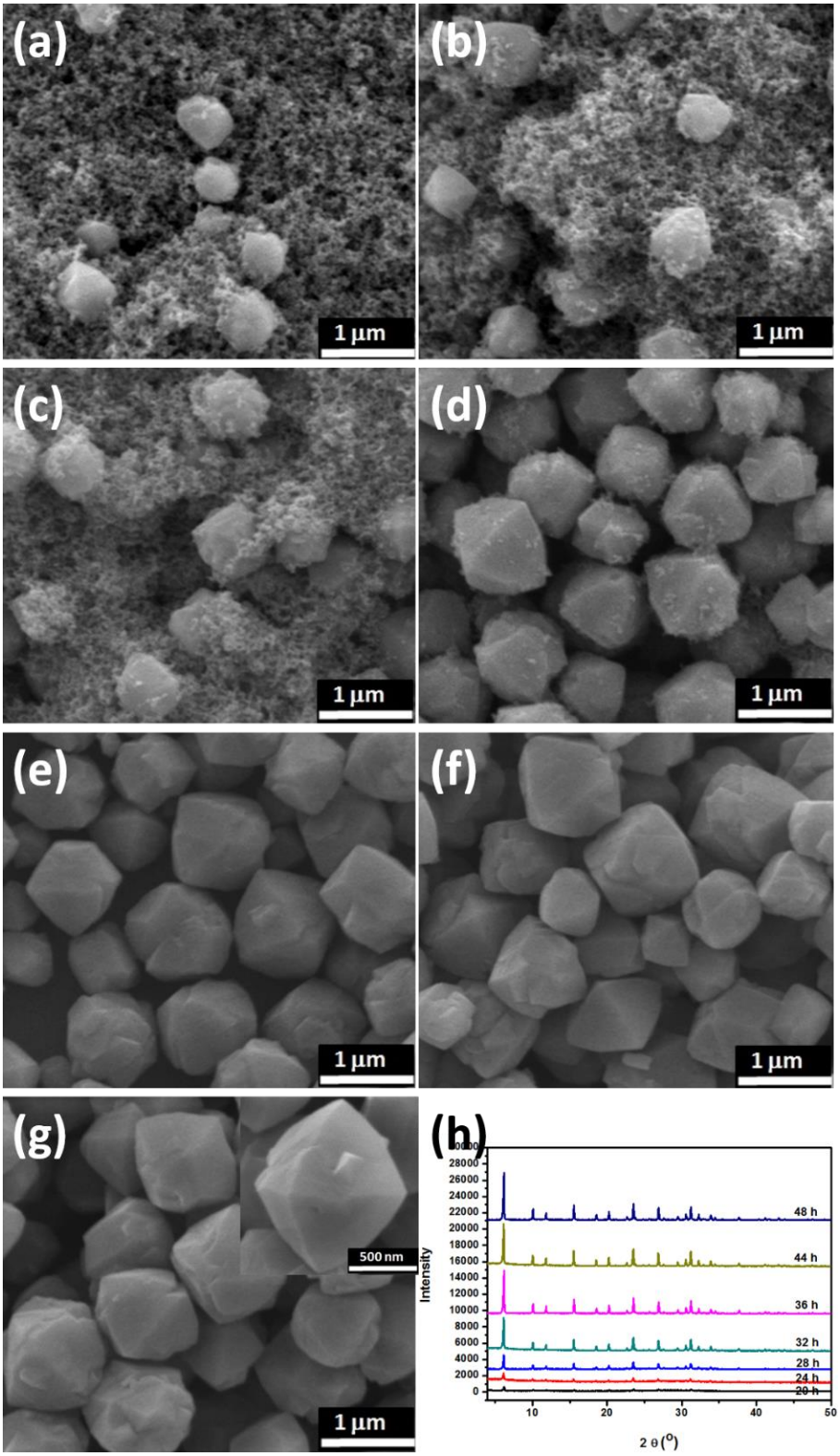

Figure S7. SEM images of CFAU samples at different synthesis stage of (a) 20 h, (b) 24 h, (c) 28 h, (d) 32 h, (e) 36 h, (f) 44 h, (g) 48 h, and (h) XRD patterns related to the samples of (a-g). The inset image in (g) at higher magnification show surface features of samples.

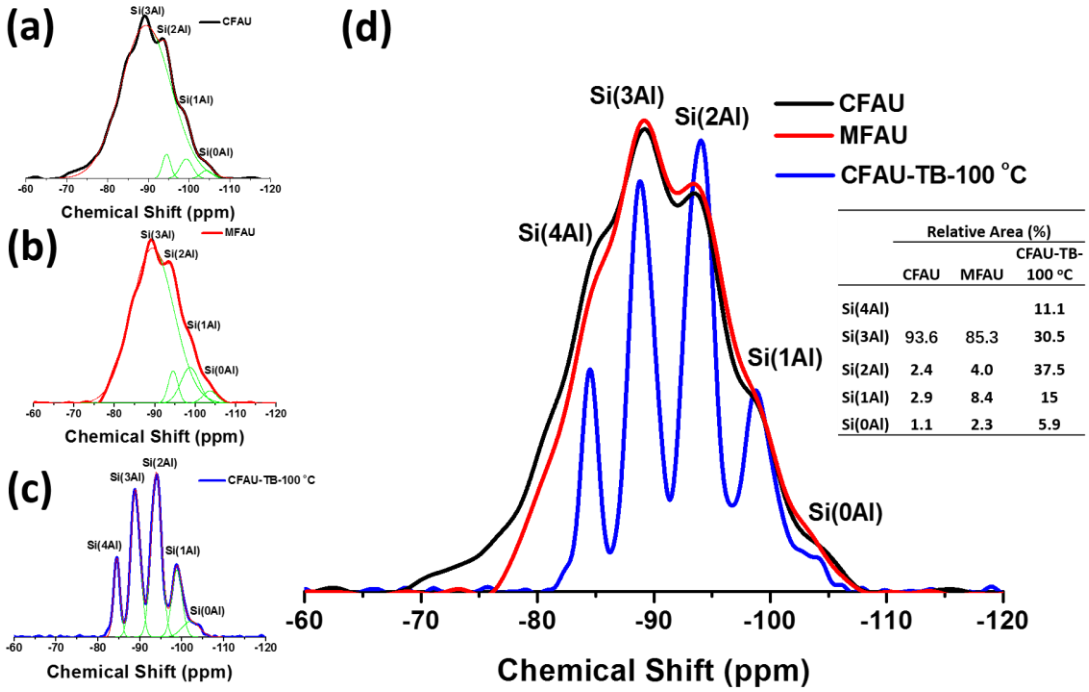

	Relative Area (%)		
	CFAU	MFAU	CFAU-TB-100 °C
Si(4Al)			11.1
Si(3Al)	93.6	85.3	30.5
Si(2Al)	2.4	4.0	37.5
Si(1Al)	2.9	8.4	15
Si(0Al)	1.1	2.3	5.9

Figure S8. ^{29}Si MAS NMR spectra of (a) CFAU crystallized at 75 °C for 20 h in the absence of organics, (b) MFAU-TB samples crystallized at 75 °C for 20 h in the presence of *tert*-butanol, (c) CFAU-TB-100 °C sample crystallized at 100 °C for 20 h in the presence of *tert*-butanol. The green curves are the deconvoluted patterns showing Q^4 silicon species coordinated with *n* OAl bonds (where *n*=0, 1, 2, and 3). (d) Overall comparison of the ^{29}Si MAS NMR spectra, inset table shows the relative peak area percentage of Si(*n*Al) species of these samples.

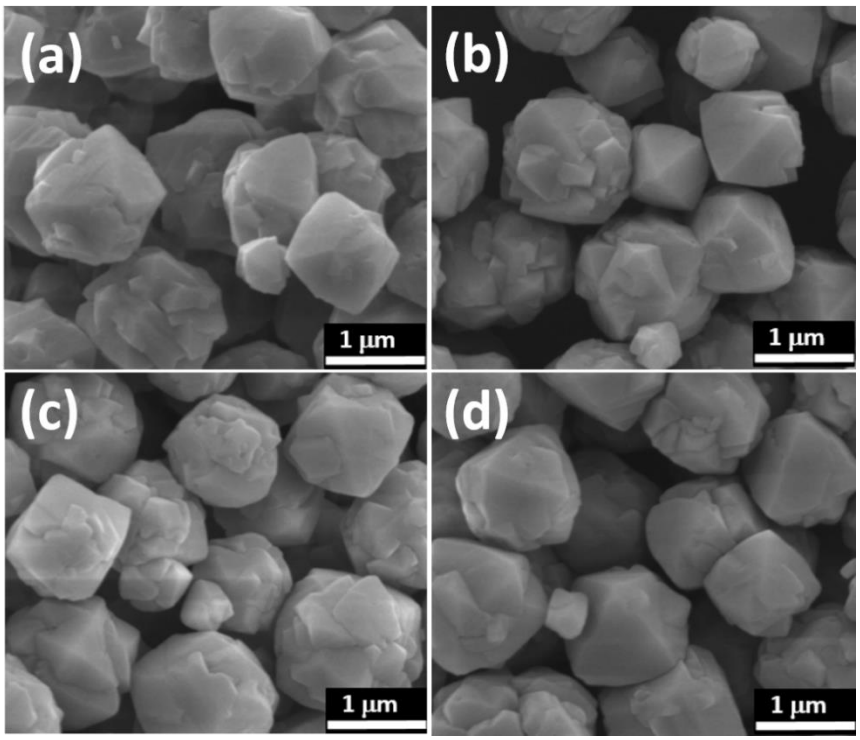

Figure S9. SEM images of FAU samples synthesized with *tert*-butanol at a temperature of 100 °C at different synthesis stage of (a) 12 h, (b) 20 h, (c) 24 h, (d) 28 h.

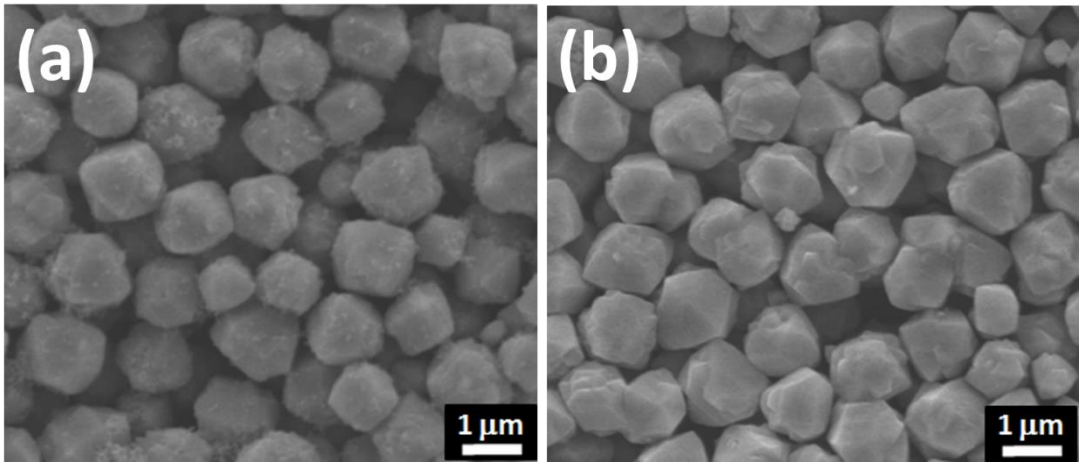

Figure S10. SEM images of FAU samples synthesized in the presence of (a) ethylene glycol, (b) glycerol.

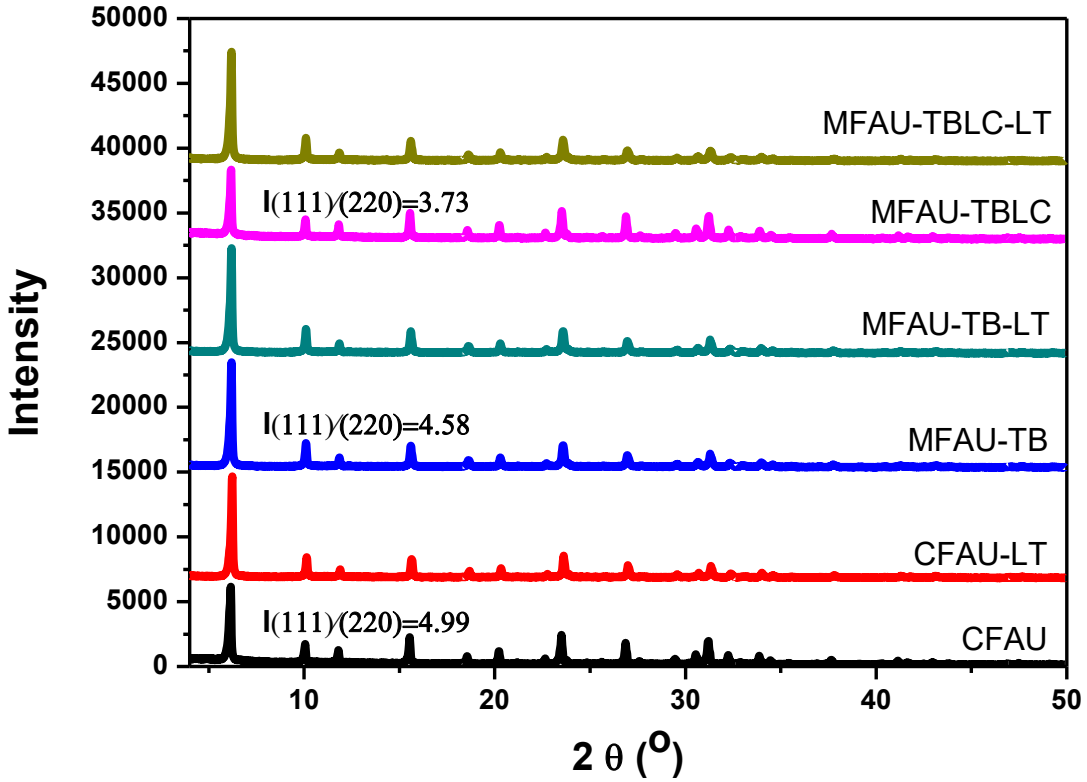

Figure S11. XRD patterns of as-made samples in this work. I(111)/(220) is the (intensity of (111) face diffraction at 2θ of 6.24°)/(intensity of (220) face diffraction at 2θ of 10.03°) from XRD patterns.

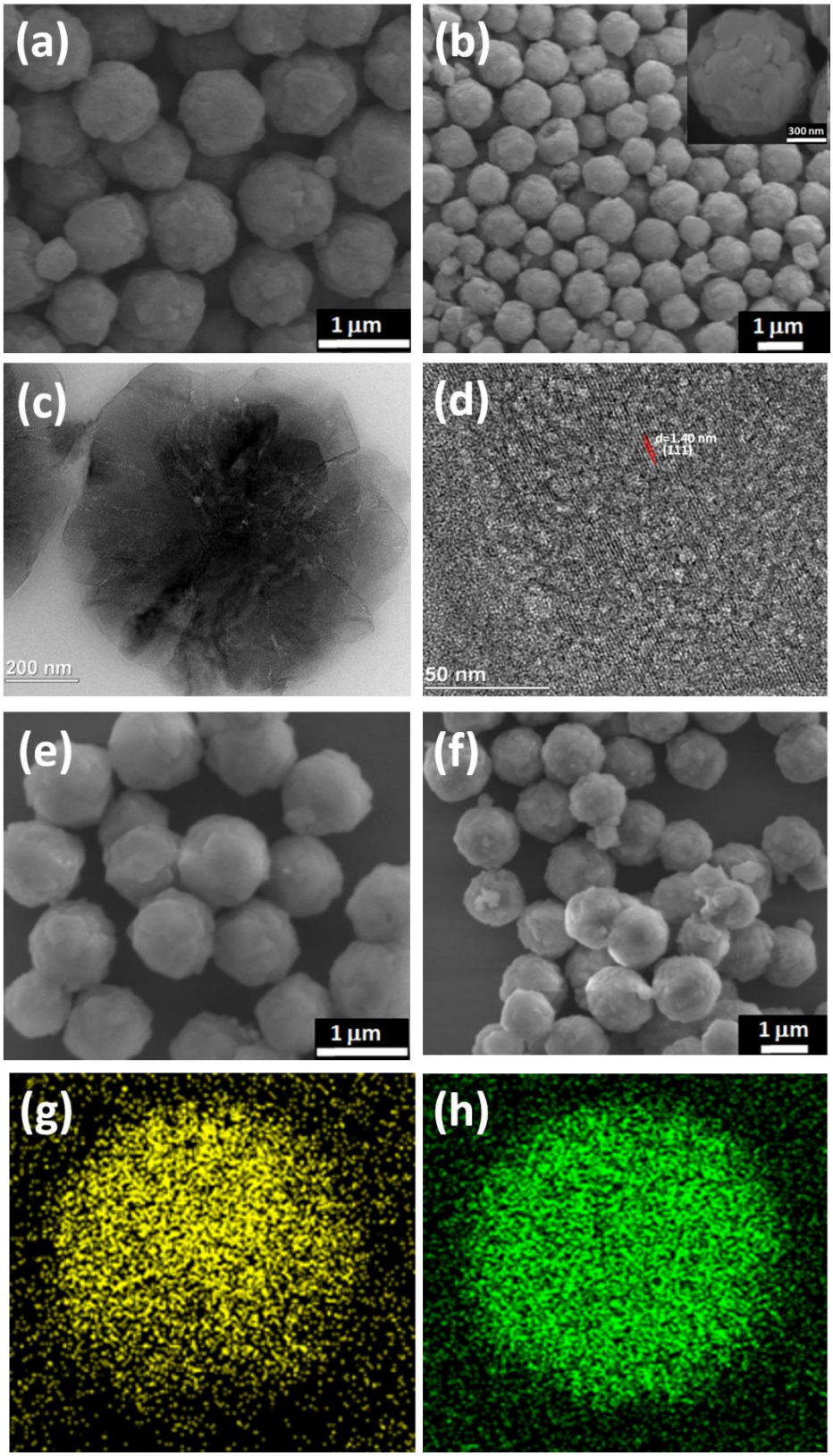

Figure S12. (a) SEM image of sample MFAU-TB. (b) SEM image, (c) low-resolution TEM, and (d) high-resolution TEM images of MFAU-TB-LT. (e-f) SEM image of sample MFAU-TB-LT-Pd^{2+} and MFAU-TBLC-LT-Pd^{2+}, (g-h) SEM-EDX mapping of sample in (f) showing element distribution of (g) Pd, (h) Al.

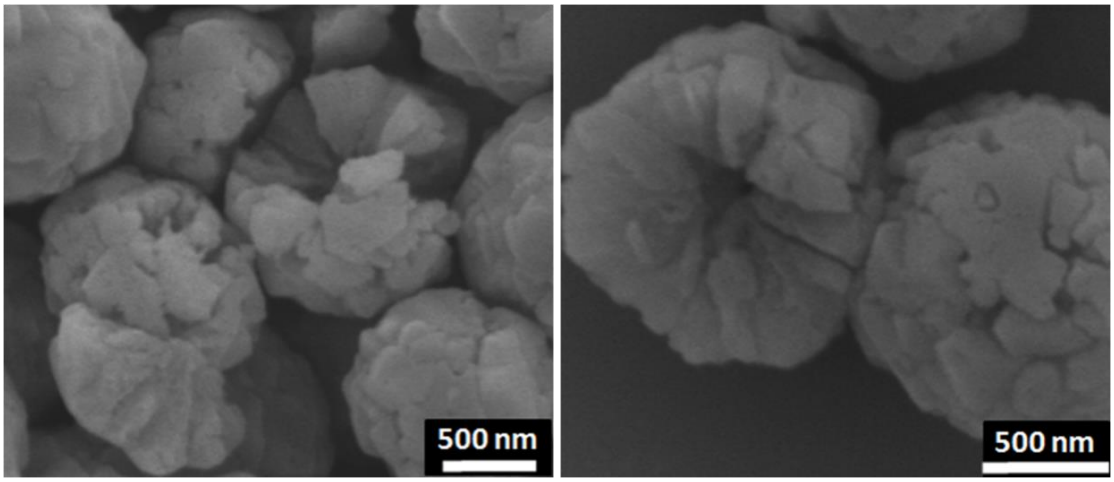

Figure S13. SEM images of occasionally cracked MFAU-TBLC-LT microsphere samples which show the wheel-like mesoporous channels.

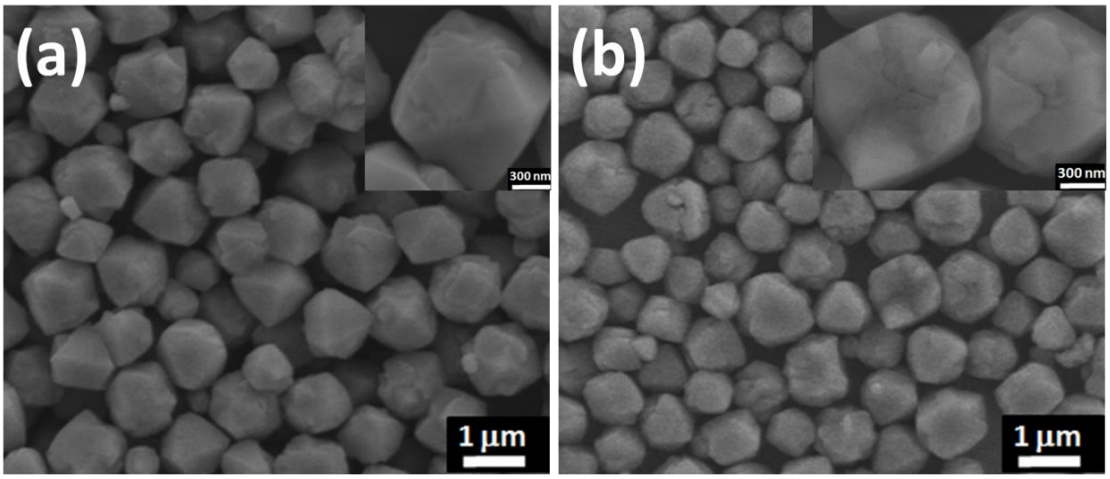

Figure S14. SEM images of (a) CFAU-LC (b) CFAU-LC-LT samples, the inset images at higher magnification show surface feature and internal architecture of samples.

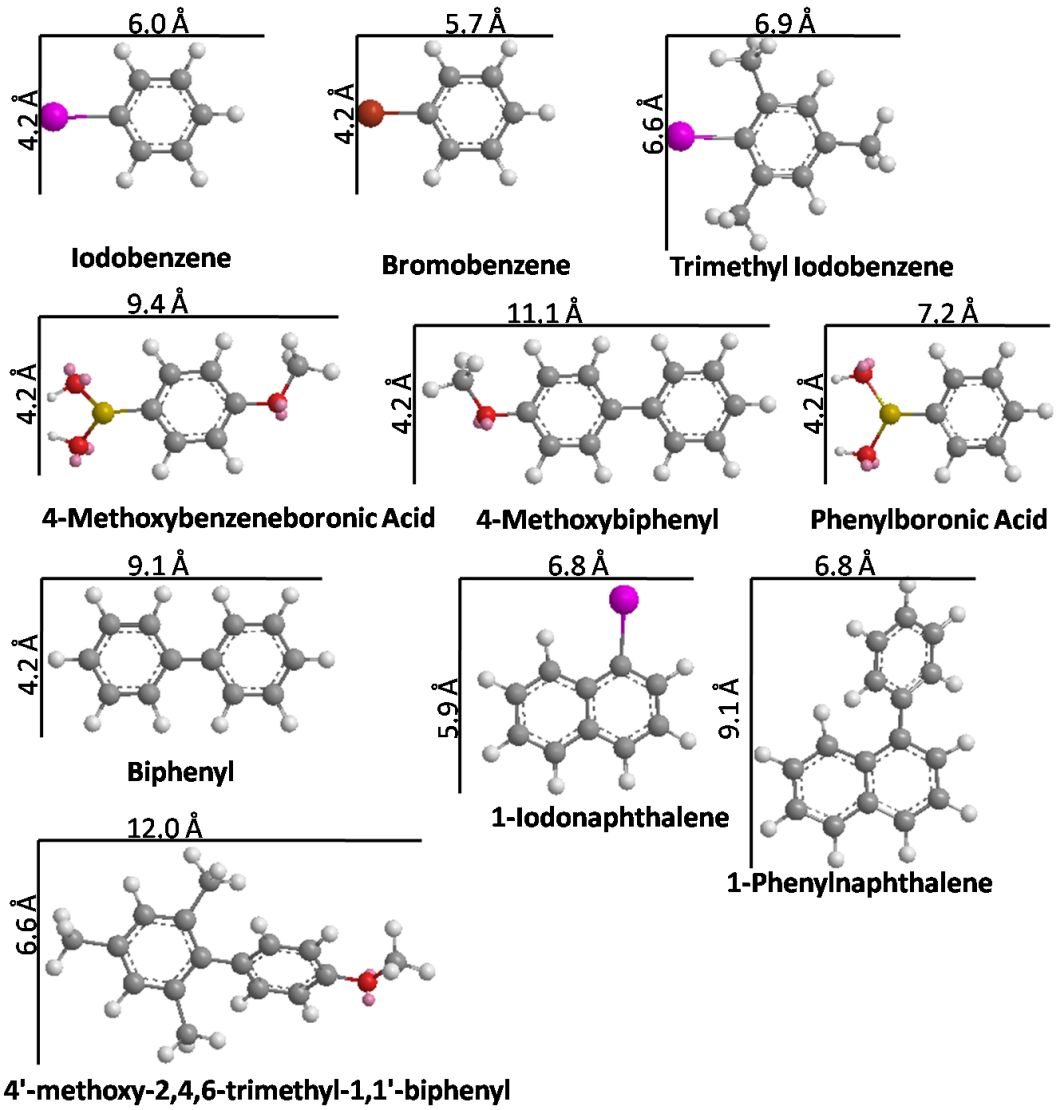

Figure S15. Sizes of different reactants and products, size measurement was made by ChemBioDraw Ultra 14.0.

Table S4. Influence of stirring rate and heterogeneous Pd catalysts on the C-C coupling reaction between bromobenzene and 4-methoxyphenylboronic acids

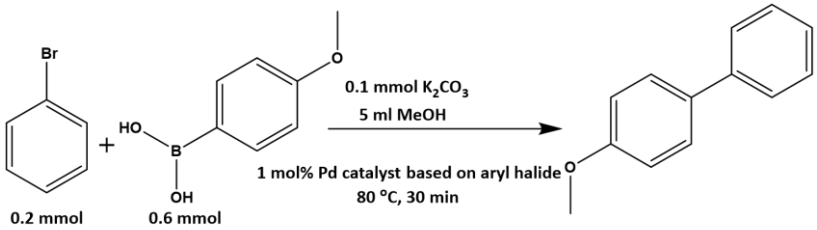

Catalyst	Yield (%)[a]		
	0 rpm	200 rpm	1000 rpm
CFAU-Pd^{2+}	58	64[b]	81
MFAU-TBLC-LT-Pd^{2+}	78	97	95
MFAU-TBLC-LT-Pd^{0}	--	52[c]	--

[a] Yield was determined by GC analysis using commercial 4-methoxybiphenyl as external standard. [b] The reaction yield was different from that shown in Table 1 when the reaction was performed in a separate set of experiment, indicating that the C-C coupling catalyzed by CFAU-Pd^{2+} was more sensitive to operation conditions and could vary from batch to batch while yield by MFAU-TBLC-LT-Pd^{2+} almost did not change at different stirring rate or different batches. [c] 13 mg MFAU-TBLC-LT-Pd^{0} zeolite was used as the coupling catalyst.

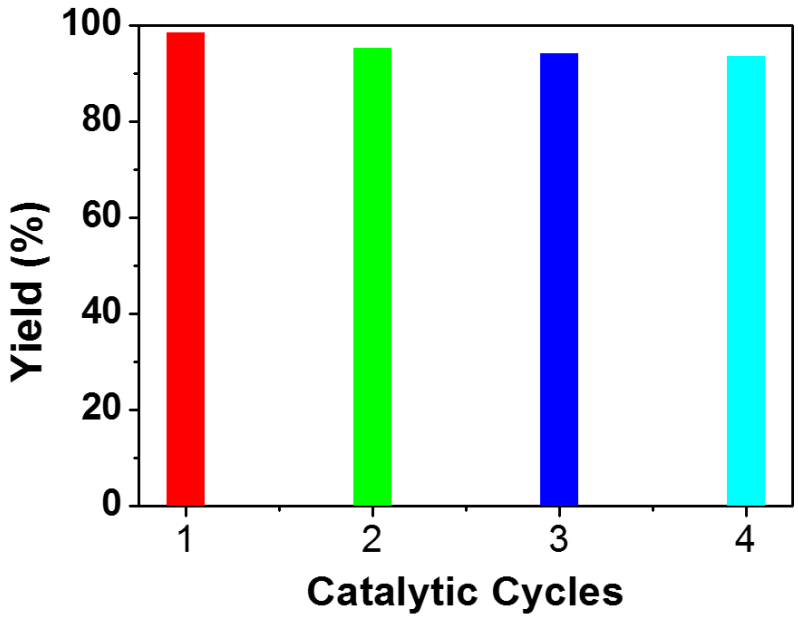

Figure S16. Reusability experiments of MFAU-TBLC-LT-Pd^{2+} during the Suzuki-Miyaura coupling reaction (entry i of Table 1). Reaction condition: 0.2 mmol **1**, 0.6 mmol **2**, 1 mol% Pd catalyst based on **1**, 0.2 mmol K_2CO_3, 5 ml MeOH, 80 °C, 30 min.

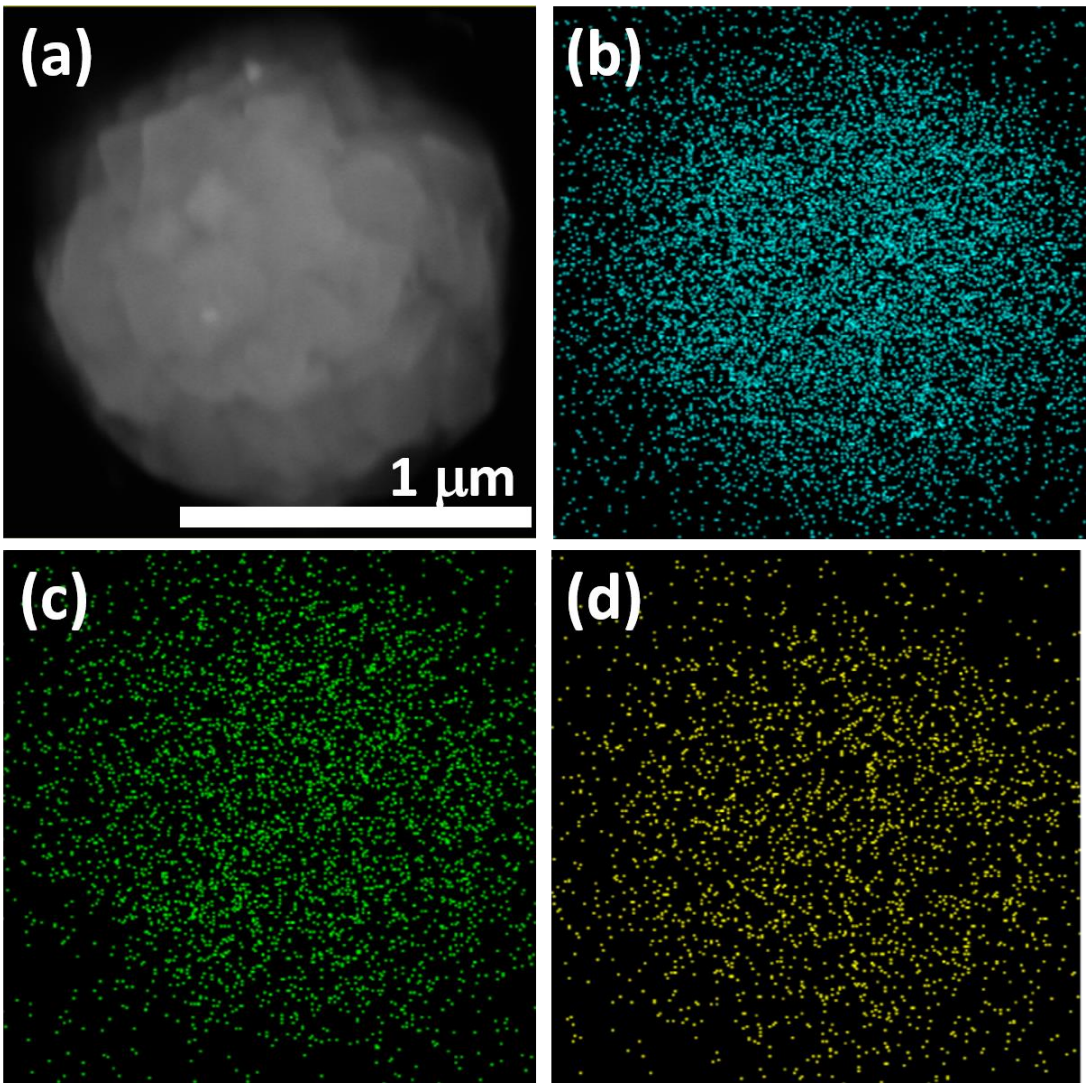

Figure S17. (a) SEM image of sample Ag@MY. (b-d) SEM-EDX mapping of sample in (a) showing element distribution of (b) Si, (c) Al, (d) Ag.

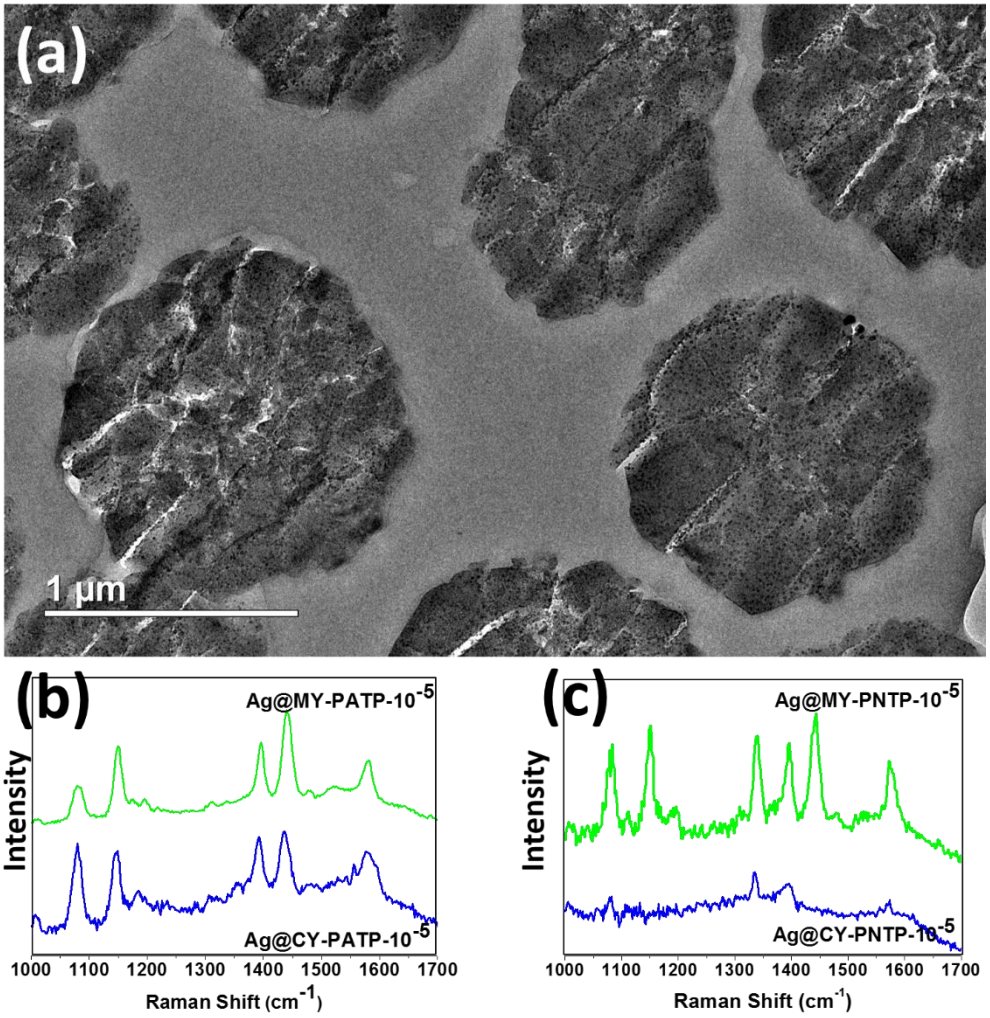

Figure S18. (a) TEM image of Ag@MY at low magnification, (b) SERS of 10^{-5} M PATP solution with Ag@MY and Ag@CY, (c) SERS of 10^{-5} M PNTP solution with Ag@MY and Ag@CY.